Heat and Mass Transfer 39 (2003) 297–304
DOI 10.1007/s00231-002-0400-1

Unsteady mixed convection flow from a rotating vertical cone with a magnetic field

H.S. Takhar, A.J. Chamkha, G. Nath

Abstract An analysis is developed to study the unsteady mixed convection flow over a vertical cone rotating in an ambient fluid with a time-dependent angular velocity in the presence of a magnetic field. The coupled nonlinear partial differential equations governing the flow have been solved numerically using an implicit finite-difference scheme. The local skin friction coefficients in the tangential and azimuthal directions and the local Nusselt number increase with the time when the angular velocity of the cone increases, but the reverse trend is observed for decreasing angular velocity. However, these are not mirror reflection of each other. The magnetic field reduces the skin friction coefficient in the tangential direction and also the Nusselt number, but it increases the skin friction coefficient in the azimuthal direction. The skin friction coefficients and the Nusselt number increase with the buoyancy force.

Keywords Unsteady mixed convection, Magnetic effects

Nomenclature

Roman letters

C_{fx}	skin friction coefficient in the x-direction
C_{fy}	skin friction coefficient in the y-direction
C_p	specific heat at constant pressure, kJôñkg^{ã1}ôñK
Ec	Eckert number
$\boldsymbol{E}$	electric field
f	dimensionless stream function
G, H	similarity velocity functions, môñs^{ã1}
Gr	Grashof number
H, h	total enthalpy and static enthalpy, respectively
Ha	Hartman number
k	thermal conductivity, $W \cdot m^{-1} \cdot K$
M	magnetic parameter
Ma	Mach number
L	characteristic length, m
Nu	Nusselt number
Pr	Prandtl number
Re	Reynolds number
St	Stanton number
t	dimensional time
t*	dimensionless time
T	temperature, K
u, v, w	velocity components, môñs^{ã1}
V	characteristic velocity, môñs^{ã1}
x, y, z	curvilinear coordinates system

Greek letters

C_{fx}	skin friction coefficient in the x-direction
α	semi-angle of the cone
β	pressure gradient parameter
γ	ratio of specific heats
η, ξ	transformed co-ordinates
μ	dynamic viscosity, $kg \cdot m^{-1} \cdot s^{-1}$
ν	konematic viscosity, $m^2 \cdot s^{-1}$
γ	density, $kg \cdot m^{-3}$
ψ	dimensional stream function, $m^2 \cdot s^{-1}$
Ω	angular velocity of the cone
Ω_0	angular velocity of the cone at t=0
φ(t)	a continuous function of time

Subscripts

i	initial conditions at the wall
w	condition at the wall
∞	condition in the free stream

Received: 3 April 2001
Published online: 29 November 2002

H.S. Takhar (✉)
Department of Engineering, Manchester Metropolitan University, Manchester, M1 5GD, U.K
E-mail: h.s.takhar@mmu.ac.uk

A.J. Chamkha
Department of Mechanical Engineering,
Kuwait University, P.O. Box. 5969, Safat 13060, Kuwait

G. Nath
Department of Mathematics,
Indian Institute of Science, Bangalore, India

1 Introduction

The study of flow and (or) heat transfer over a rotating body has several practical applications. Such a study is important in the design of turbines and turbo-machines, in estimating the flight path of rotating wheels and spin-stabilized missiles and in the modelling of many geophysical vortices. When an axisymmetric body rotates in a forced flow field, the fluid near the surface of the body is forced outward in the radial direction due to the action of the centrifugal force. This fluid is then replaced by the fluid moving in the axial direction. Thus the axial velocity of the fluid in the vicinity of a rotating body is higher than that of a stationary body. This increase in the axial velocity enhances the convective heat transfer between the body and

the fluid. This principle has been used to develop practical systems for increasing heat transfer. For example, Hickman [1] showed the utility of rotating condensers for sea-water distillation and space-craft power plants in a zero-gravity environment. Ostrach and Braun [2] investigated the possibility of cooling the nose-cone of re-entry vehicles by spinning the nose. Rotating heat exchangers are extensively used by the chemical and automobile industries. The investigation of flow and heat transfer in rotating systems done prior to 1958 has been reported by Dorfman [3], while Kreith [4] reviewed the work done up to 1968.

The problem of forced convection from isothermal and non-isothermal disks rotating in an ambient fluid was investigated by Sparrow and Gregg [5] and Hartnett [6], respectively. Tien and Tsugi [7], and Koh and Price [8] have presented a theoretical analysis of the forced flow and heat transfer past a rotating cone. The influence of the Prandtl number on the heat transfer on rotating non-isothermal disks and cones was investigated by Hartnett and Deland [9]. The effect of the axial magnetic field on the flow and heat transfer over a rotating disk was considered by Sparrow and Cess [10]. Tarek et al. [11] have obtained an asymptotic solution of the flow problem over a rotating disk with a weak axial magnetic field. Lee et al. [12] have studied the flow and heat transfer over a rotating body of revolution (sphere). Wang [13] has investigated the flow and heat transfer on rotating cones, disks and axi-symmetric bodies with concentrated heat sources. The similarity solution of the mixed convection from a rotating vertical cone in an ambient fluid was obtained by Hering and Grosh [14] for Prandtl number Pr = 0.7 and by Himasekhar et al. [15] for a wide range of Prandtl numbers. Thacker et al. [16] have studied the free convection from a disk rotating in a vertical plane in the presence of an axial magnetic field. All these studies deal with steady flows. In many practical problems, the flow could be unsteady due to the angular velocity of the spinning body which varies with time or due to the impulsive change in the angular velocity of the body. The unsteady boundary layer flow of an impulsively-started translating and spinning rotational symmetric body has been investigated by Ece [17], who obtained the solution for small time. The corresponding heat transfer problem has been considered by Ozturk and Ece [18]. The general tendency of the positive buoyancy force is to increase the heat transfer while the magnetic field tends to reduce it. Further the reduction of the angular velocity of the body with increasing time also reduces the heat transfer. Therefore it is interesting as well as useful to study the combined effects of the buoyancy force and the magnetic field on a rotating body where the angular velocity decreases with increasing time.

In this paper, we have studied the unsteady mixed convection flow over a rotating vertical cone in the presence of a magnetic field. The unsteadiness in the flow field is due to the angular velocity of the cone which varies arbitrarily with time. The coupled nonlinear parabolic partial differential equations governing the mixed convection flow have been solved numerically using an implicit finite-difference scheme similar to that of Blottner [19]. The steady-state results for the surface shear stresses and heat transfer are compared with those of Himasekhar et al. [15] and Sparrow and Cess [10]. One possible application of this work is in nuclear reactors where the cooling process can be made more efficient by the combined effects of the magnetic field and the time-dependent rotation of the body. Another possible application is in the cooling of the nose-cone of a re-entry vehicle by the rotation of the cone.

2 Analysis

Let us consider the unsteady, laminar, non-dissipative, constant property, incompressible boundary-layer mixed convection flow of an electrically-conducting fluid over a heated vertical cone rotating in an ambient fluid with time-dependent angular velocity, $\Omega(t^*) = \Omega_0\varphi(t^*)$, $t^* = (\Omega_0 \sin \alpha)\, t$, around the axis of the cone. The magnetic field B is applied in the z-direction (normal direction) and the gravity g acts downward parallel to the axis of the cone. The physical model and the coordinate system are shown in Fig. 1. We have employed the rectangular curvilinear fixed coordinate system (x, y, z), where x is measured along a meridional section, the y-axis is along a circular section, and the z-axis is normal to the cone surface. Let u, v and w be the velocity components along the x (tangential), y (circumferential or azimuthal) and z (normal) directions, respectively. The wall temperature T_w varies linearly with the distance x and the ambient temperature T_∞ is a constant. The cone surface is assumed to be electrically-insulated. Also the flow is taken to be axisymmetric. The magnetic Reynolds number is assumed to be small ($Re_m = \mu_0\sigma$ VL $\ll 1$ where μ_0 and σ are the magnetic permeability and the electrical conductivity, and V and L are the characteristic velocity and length, respectively). Under these conditions, it is possible to neglect the induced magnetic field in comparison to the applied magnetic field. Since there is no applied or polarization voltage imposed on the flow field, the electric field $\mathbf{E} = 0$. Hence, only the magnetic field

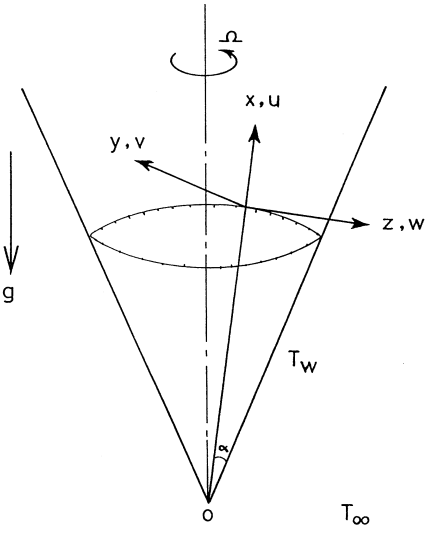

Fig. 1. Physical model and coordinates system

contributes towards the Lorentz force. Under the above assumptions and using the Boussinesq approximation, the boundary-layer equations governing the mixed convection flow on the rotating cone [7, 10, 15, 20] are given by;

$$\text{Continuity:}\quad u_x + x^{-1}u + w_z = 0, \tag{1}$$

Momentum:

$$u_t + uu_x + wu_z - v^2/x = \nu u_{zz} + g\beta\cos\alpha(T - T_\infty) - \sigma B^2 u/\rho, \tag{2}$$

$$v_t + uv_x + wv_z + uv/x = \nu v_{zz} - \sigma B^2 v/\rho, \tag{3}$$

$$\text{Energy:}\quad T_t + uT_x + wT_z = (\nu/\mathrm{Pr})T_{zz}. \tag{4}$$

The initial conditions are given by the steady-state equations;

$$\begin{aligned} u(x,z,0) = u_i(x,z), v(x,z,0) = v_i(x,z), w(x,z,0) \\ = w_i(x,z), T(x,z,0) = T_i(x,z). \end{aligned} \tag{5}$$

The boundary conditions on the surface are the no-slip conditions and far away from the surface the conditions are given by the ambient conditions;

$$\begin{aligned} &u(x,0,t) = w(x,0,t) = 0,\ v(x,0,t) = \Omega_0 x\sin\alpha\,\phi(t^*), \\ &T(x,0,t) = T_w(x), \\ &u(x,\infty,t) = v(x,\infty,t) = 0,\ T(x,\infty,t) = T_\infty, \\ &u(\infty,z,t) = v(\infty,z,t) = 0,\ T(\infty,z,t) = T_\infty,\ z > 0. \end{aligned} \tag{6}$$

Here T is the temperature; β is the coecient of the volumetric expansion; α is the semi-vertical angle of the cone; ν is the kinematic viscosity; γ is the density of the fluid; t and t*(t* = Ω_0t sinα) are the dimensional and dimensionless times, respectively; Ω_0 is the angular velocity of the cone at t = 0; Pr is the Prandtl number; φ(t) is a continuous function having a continuous first-order derivative; the subscripts t, x and z denote partial derivatives with respect to t, x and z, respectively; the subscript i denotes initial conditions; and the subscripts w and ∞ denote wall and ambient conditions, respectively.

It is convenient to transform Eqs.(1, 2, 3, 4) into the (η, t*) system by applying the following transformations;

$$\begin{aligned} &\eta = (\Omega_0\sin\alpha/\nu)^{1/2}z,\ t^* = (\Omega_0 x\sin\alpha)t,\ u(x,z,t) \\ &\quad = -2^{-1}(\Omega_0\sin\alpha)H'(\eta,t^*)\phi(t^*), \\ &v(x,z,t) = (\Omega_0 x\sin\alpha)G(\eta,t^*)\phi(t^*),\ w(x,z,t) \\ &\quad = (\nu\Omega_0\sin\alpha)^{1/2}H(\eta,t^*)\phi(t^*), \\ &T(x,z,t) - T_\infty = (T_{w0} - T_\infty)\theta(\eta,t^*),\ T_W - T_\infty \\ &\quad = (T_{w0} - T_\infty)x/L, \\ &Gr_L = g\beta\cos\alpha(T_w - T_\infty)L^3/\nu^2,\ Re_L = \Omega_0 L^2\sin\alpha/\nu, \\ &\lambda = Gr_L/Re_L^2, \\ &M = H_a/Re_L,\ H_a = \sigma B^2 L^2/\mu, \end{aligned} \tag{7}$$

where T_{w0} is the wall temperature at time t*=0. We find that Eq.(1) is identically satisfied and Eqs.(2, 3, 4) reduce to the following system of equations,

$$\begin{aligned} H''' - \phi HH'' + 2^{-1}\phi(H')^2 - 2\phi G^2 - 2\phi^{-1}\lambda\theta - MH' \\ - \phi^{-1}(d\phi/dt^*)H' - \partial H'/\partial t^* = 0, \end{aligned} \tag{8}$$

$$G'' - \phi(HG' - H'G) - (M + \phi^{-1}d\phi/dt^*)G - \partial G/\partial t^* = 0, \tag{9}$$

$$\theta'' - \mathrm{Pr}(H\theta' - 2^{-1}H'\theta)\phi - \mathrm{Pr}\,\partial\theta/\partial t^* = 0. \tag{10}$$

The boundary conditions (6) can be rewritten as;

$$\begin{aligned} &H(0,t^*) = H'(0,t^*) = 0, \quad G(0,t^*) = \theta(0,t^*) = 1, \\ &H'(\infty,t^*) = G(\infty,t^*) = \theta(\infty,t^*) = 0. \end{aligned} \tag{11}$$

The initial conditions (i.e., conditions at t* = 0) are given by the steady state equations obtained from (8, 9, (10) by putting φ =1, dφ/dt* = $\partial\dot{H}/\partial t^*$ = $\partial G/\partial t^*$ = 0 when t* = 0. The steady-state equations are;

$$H''' - HH'' + 2^{-1}(H')^2 - 2G^2 - 2\lambda\theta - MH' = 0, \tag{12}$$

$$G'' - (HG' - H'G) - MG = 0, \tag{13}$$

$$\theta'' - \mathrm{Pr}(H\theta' - 2^{-1}H'\theta) = 0, \tag{14}$$

with boundary conditions

$$\begin{aligned} H(0) = H^{/}(0) = 0, G(0) = \theta(0) = 1, H^{/}(\infty) = G^{/}(\infty) \\ = \theta^{/}(\infty) = 0. \end{aligned} \tag{15}$$

Here η and t* are the transformed coordinates; H′, G and H are the dimensionless velocity components along the tangential, azimuthal and normal directions, respectively; ö¡ is the dimensionless temperature; Gr_L is the Grashof number; Re_L is the Reynolds number; λ is the dimensionless buoyancy parameter; M is the dimensionless magnetic parameter; H_a is the Hartmann number; L is the characteristic length; μ is the coefficient of viscosity; and a prime denotes a derivative with respect to η. Here we have taken a linear variation of the wall temperature T_w with the distance x, because the governing equations(8, 9, 10) become independent of x. Hence the number of independent variables becomes two instead of three.

It may be remarked that the steady-state Eqs.(12, 13, 14) in the absence of the magnetic field (M = 0) are identical to those of Himasekhar et al. [15] if we replace H′ by -2F and λ by Gr/Re^2. Further, Eqs.(12, 13, 14) in the absence of the buoyancy force (λ = 0) and for the constant wall temperature case are the same as those of Sparrow and Cess [10] if we omit the term Pr H′ θ/2, which is the contribution due to the linear variation of the wall temperature with the distance x.

The quantities of physical interest are the local skin friction coefficients in the tangential and azimuthal directions and the local heat transfer coefficient in terms of Nusselt number and these are given by;

$$C_{fx} = 2\mu(\partial u/\partial z)_{z=0}/[\rho(\Omega_0 x \sin\alpha)^2] = Re_x^{-1/2}\phi(t^*)H''(0,t^*),$$

$$C_{fy} = -2\mu(\partial v/\partial z)_{z=0}/[\rho(\Omega_0 x \sin\alpha)^2]$$

$$= -Re_x^{-1/2}\phi(t^*)G'(0,t^*),$$

$$Nu_x = -x(\partial T/\partial z)_{z=0}/(T_w - T_\infty) = -Re_x^{1/2}\theta(0,t^*), \quad (16)$$

where C_{fx} and C_{fy} are the local skin friction coecients in the tangential and azimuthal directions, respectively; Nu_x is the local Nusselt number; and Re_x ($Re_x = \Omega_0 x^2 \sin\alpha/\nu$) is the local Reynolds number. Here both the coecients and the Reynolds number are based on the initial velocity.

3
Method of solution

The coupled nonlinear parabolic partial differential Eqs.(8, 9, 10) under boundary conditions (11) and initial conditions (12, 13, 14, 15) have been solved numerically using an implicit, iterative tri-diagonal finite-difference scheme similar to that of Blottner [19]. All the first-order derivatives with respect to t* are replaced by two-point backward difference formulae of the form,

$$\partial R/\partial t^* = (R_{i,j} - R_{i-1,j})/\Delta t^* \quad (17)$$

where R represents the dependent variables H or G or θ and i and j are node locations in the t* and η directions, respectively. First, the third-order partial dierential Eq.(8) is converted into a second-order partial dierential equation by substituting H′ = N. Then the second-order partial dierential equations for N, G and θ are discretized using three-point central dierence formulae, while first-order derivatives with respect to η are discretized by employing the trapezoidal rule. At each line of constant t*, we get a system of algebraic equations. We evaluate the nonlinear terms at the previous iteration and solve the system of algebraic equations iteratively by using the Thomas algorithm (see Blottner [19]). The same procedure is repeated for the next t* value and the problem is solved line by line until the desired t* value is reached. A convergence criterion based on the relative dierence between the current and previous iterations is employed. When this dierence reaches 10^{-5}, the solution is assumed to have converged and the iterative process is terminated.

4
Results and discussion

The partial differential Eqs.(8, 9, 10) under the boundary conditions (11) and the initial condition Eqs.(12, 13, 14, 15) are solved numerically by using an implicit finite-difference method described earlier. The results have been obtained for both increasing and decreasing angular velocities ($\varphi(t^*) = 1 + \varepsilon t^{*2}$, $\varepsilon = \pm 0.2$, $0 \le t^* \le 2$) for several values of the parameters λ ($0 \le \lambda \le 10$), M ($0 \le M \le 4$), and Pr ($0.7 \le Pr \le 10$).

In order to assess the accuracy of our method, we have compared the steady-state results for the surface shear stresses in the tangential and azimuthal directions ($-H''(0)$, $G'(0)$), and the surface heat transfer ($-\theta'(0)$) in the absence of the magnetic field (M = 0) with those of Himasekhar et al. [15] and found them in excellent agreement. We have also compared the surface shear stresses and heat transfer ($-H''(0)$, $-G'(0)$, $-\theta'(0)$), and ambient velocity $-H(\infty)$ for the steady-state case in the absence of the buoyancy force (λ=0) with those of Sparrow and Cess [10] and the results are found to be in very good agreement. Since the maximum difference between our results and those of refs. [10, 15] is about 1%, the comparison is not shown here.

The effect of the magnetic parameter M on the local skin friction coefficients in the tangential and azimuthal directions ($2^{-1}\ Re_x^{1/2}\ C_{fx}$, $2^{-1}\ Re_x^{1/2}\ C_{fy}$) and the local Nusselt number ($Re_x^{-1/2}\ Nu_x$) for increasing and decreasing angular velocities ($\varphi(t^*) = 1 + \varepsilon t^*$, $\varepsilon = \pm 0.2$) when $\lambda = 1$, Pr = 0.7, $0 \le t^* \le 2$ is shown in Figs.2, 3, 4, respectively. The effect of the time variation is more pronounced for large t*(t* > 1). For a fixed M, the skin friction coefficients and the Nusselt number increase with an increasing angular velocity, but the reverse trend is observed for a decreasing angular velocity. However, these are not a mirror reflection of each other. When the angular velocity increases with time, the skin-friction coefficients ($2^{-1}\ Re_x^{1/2}\ C_{fx}$, $2^{-1}\ Re_x^{1/2}\ C_{fy}$) and the Nusselt number ($Re_x^{-1/2}\ Nu_x$) for M=2 increase by about 57%, 100%and 5.5% respectively, as t* increases from zero to 2. Since an increase in the angular velocity with time directly affects the tangential velocity, the skin friction coefficient in the tangential direction is most affected. However, the effect of an increase in the angular velocity on the energy equation is rather indirect. Hence the Nusselt number is weakly affected. When the angular velocity decreases with time, the skin friction coefficient in the tangential direction for M=0 (without the magnetic field) becomes negative for t* > 1.75. However this does not imply separation, since we are dealing with the unsteady flow. For M=4 and for

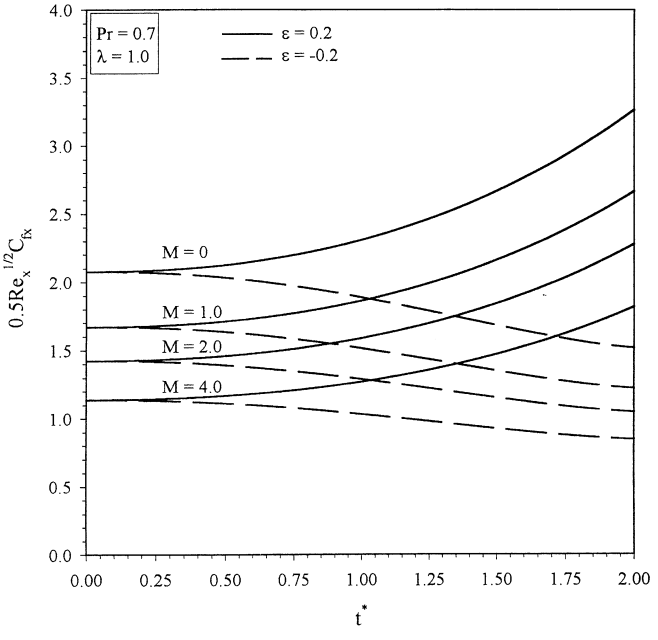

Fig. 2. Effect of the magnetic parameter M on $2^{-1}\ Re_x^{1/2}\ C_{fx}$ for $\varphi(t^*) = 1 + \varepsilon t^{*2}$, $\varepsilon = \pm 0.2$

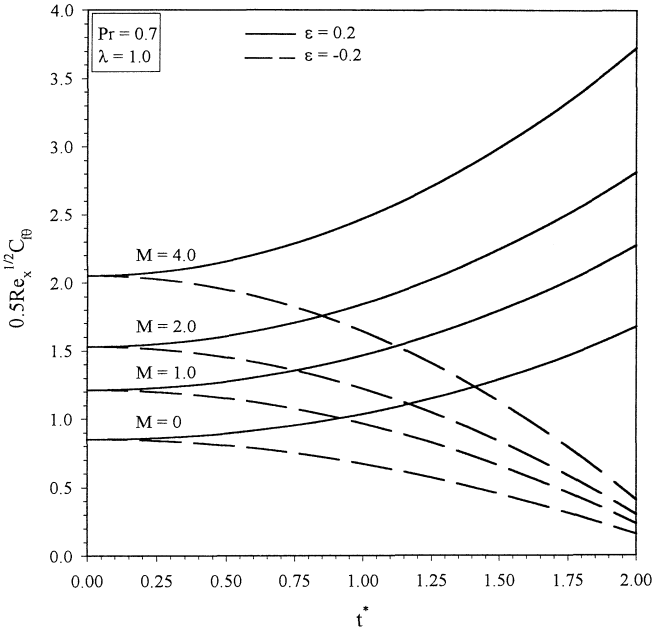

Fig. 3. Effect of the magnetic parameter M on $2^{-1}\ Re_x^{1/2}\ C_{fy}$ for $\varphi(t^*) = 1 + \varepsilon t^{*2}$, $\varepsilon = \pm 0.2$

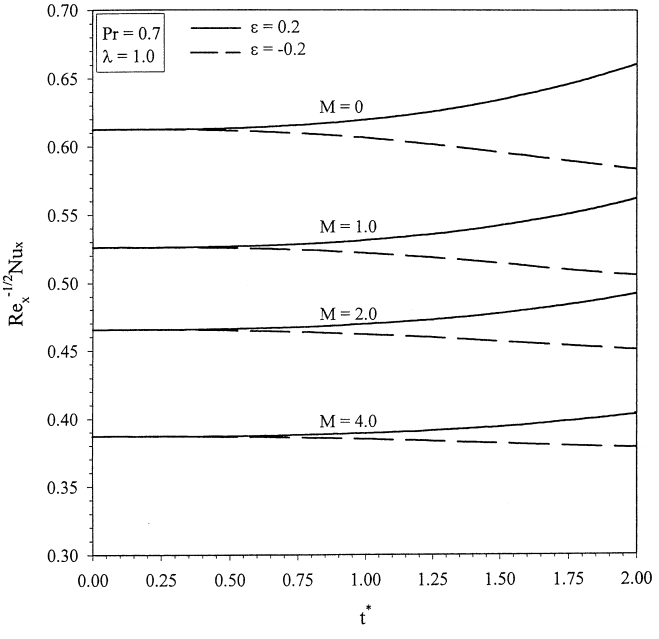

Fig. 4. Effect of the magnetic parameter M on $2^{-1}\ Re_x^{-1/2}\ Nu_x$ for $\varphi(t^*) = 1 + \varepsilon t^{*2}$, $\varepsilon = \pm 0.2$

increasing angular velocity, the skin friction coefficient in the tangential direction increases by about 88% when t* increases from zero to 2, whereas it decreases by about 93% for the decreasing angular velocity. The skin friction coefficients and the Nusselt number are found to be strongly dependent on M for all t*. The skin friction coefficient in the tangential direction ($2^{-1}\ Re_x^{1/2}\ C_{fx}$) and the Nusselt number ($Re_x^{-1/2}\ Nu_x$) decrease with increasing M, but the skin friction coefficient in the azimuthal direction ($2^{-1}\ Re_x^{1/2}\ C_{fy}$) decreases. The reason for this behaviour can be explained as follows. When the body

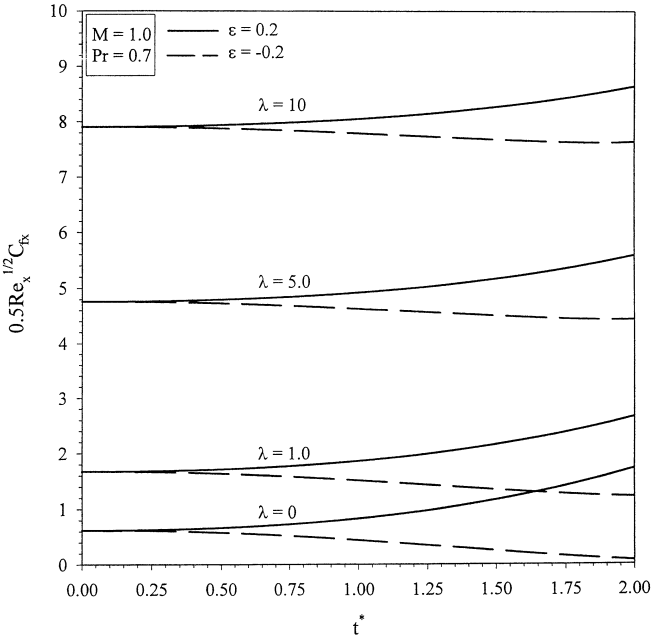

Fig. 5. Effect of the buoyancy parameter λ on $2^{-1}\ Re_x^{1/2}\ C_{fx}$ for $\varphi(t^*) = 1 + \varepsilon t^{*2}$, $\varepsilon = \pm 0.2$

rotates, fluid near the surface of the body is forced outward along the tangential direction due to the action of the centrifugal force. This fluid is then replaced by the fluid moving in the normal direction. Thus, there is a close relationship between the tangential and normal velocities. Since the magnetic field is applied normal to the velocity H, there is however, an x-component of the magnetic force (see Eq.(8)) which opposes the tangential velocity H′. The resultant reduction in the tangential velocity H′ with increasing M is reflected in the reduction of the normal velocity H (see Figs.8 and 9). Since there is less fluid flow, the change from the inflow velocity H to the outflow velocity H′ takes place closer to the surface of the cone. Thus, the inflow velocity remains constant within smaller distances from the surface as the magnetic parameter M increases. Consequently, the gradient of the velocity in the tangential direction and hence the skin friction coefficient in the tangential direction decrease with increasing M. Since the normal velocity H decreases with increasing M, as mentioned earlier, the temperature θ increases with M (see Fig.11). Hence, the temperature gradient and the Nusselt number also decrease. Since the magnetic field induces the Lorentz force in the azimuthal direction which opposes the velocity G, it is reduced everywhere and the boundary layer is thinned as M increases (see Fig.10). This results in an increase in the gradient of the velocity G and, hence, in the skin friction coefficient in the azimuthal direction with increasing M.

The effect of the buoyancy parameter λ on the local skin friction coefficient in the tangential and azimuthal directions ($2^{-1}\ Re_x^{1/2}\ C_{fx}$, $2^{-1}\ Re_x^{1/2}\ C_{fy}$) and the local Nusselt number ($Re_x^{-1/2}\ Nu_x$) is presented in Figs.5, 6, 7 for $\varphi(t^*) = 1 + \varepsilon\ t^{*2}$, $\varepsilon = \pm 0.2$, M = 1, Pr = 0.7. Since the positive buoyancy force ($\lambda > 0$) implies favourable pressure gradient, the fluid gets accelerated, which results in thinner momentum and thermal boundary layers.

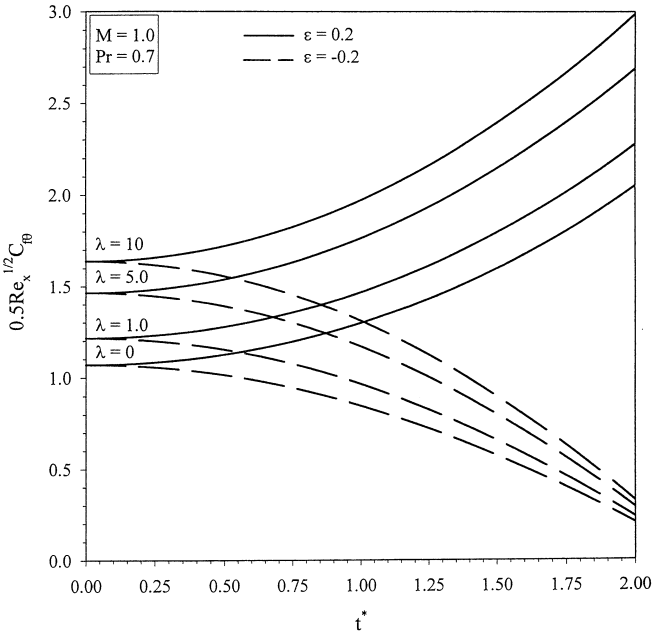

Fig. 6. Effect of the buoyancy parameter λ on 2^{-11} $Re_x^{1/2}$ C_{fy} for $\varphi(t^*) = 1 + \varepsilon t^{*2}$, $\varepsilon = \pm 0.2$

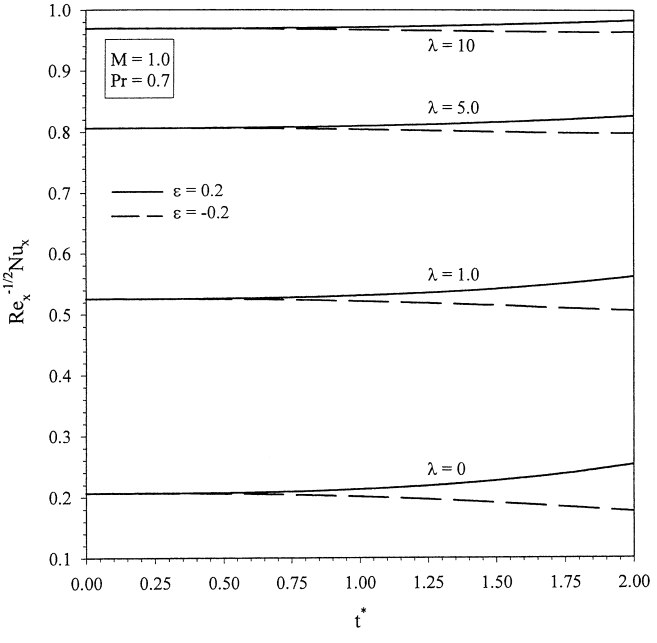

Fig. 7. Effect of the buoyancy parameter λ on $Re_x^{-1/2}$ Nu_x for $\varphi(t^*) = 1 + \varepsilon t^{*2}$, $\varepsilon = \pm 0.2$

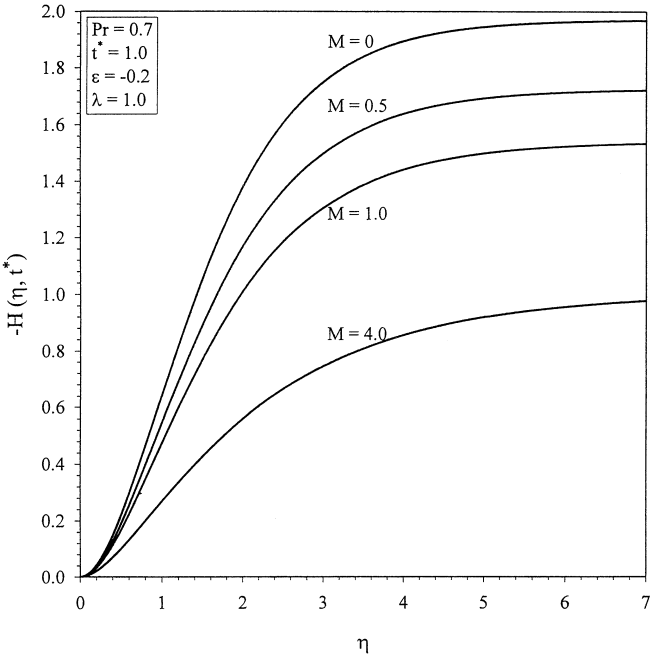

Fig. 8. Effect of M on the velocity profiles $-H(\eta, t^*)$ for $\varphi(t^*) = 1 + \varepsilon t^{*2}$, $\varepsilon = -0.2$

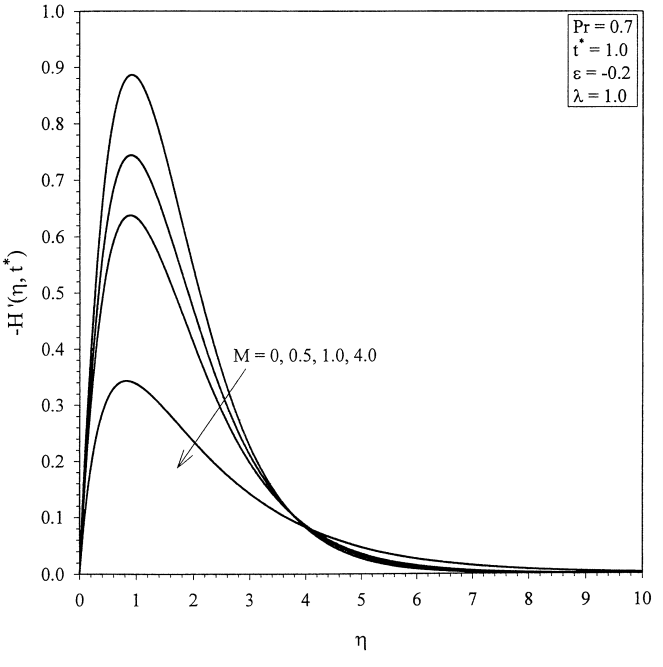

Fig. 9. Effect of M on velocity profiles $-H'(\eta, t^*)$ for $\varphi(t^*) = 1 + \varepsilon t^{*2}$, $\varepsilon = -0.2$

Consequently, the velocity and temperature gradients are increased and, hence, the skin friction coefficients and the Nusselt number also increase with λ.

The effect of the time variation is found to be more pronounced on the skin friction in the tangential direction (2^{-1} $Re_x^{1/2}$ C_{fy}) than on the skin friction coefficient in the azimuthal direction (2^{-1} $Re_x^{1/2}$ C_{fx}) and the Nusselt number ($Re_x^{-1/2}$ Nu_x), because the change in of the angular velocity with time strongly affects the tangential velocity. For λ=5, the skin friction coefficient in the tangential direction (2^{-1} $Re_x^{1/2}$ C_{fy}) increases by about 77% when the time t* increases from zero to 2. On the other hand for decreasing angular velocity, the tangential skin friction decreases by about 88% when t* increases from zero to 2. When the angular velocity decreases with time the skin friction in the tangential direction (2^{-1} $Re_x^{1/2}$ C_{fy}) < 0 when $\lambda < 1$ and $t^* > t_0^*$). However as mentioned earlier this does not imply flow separation.

The effect of the magnetic parameter M on the normal, tangential and azimuthal velocities (H, H′, G) and on the

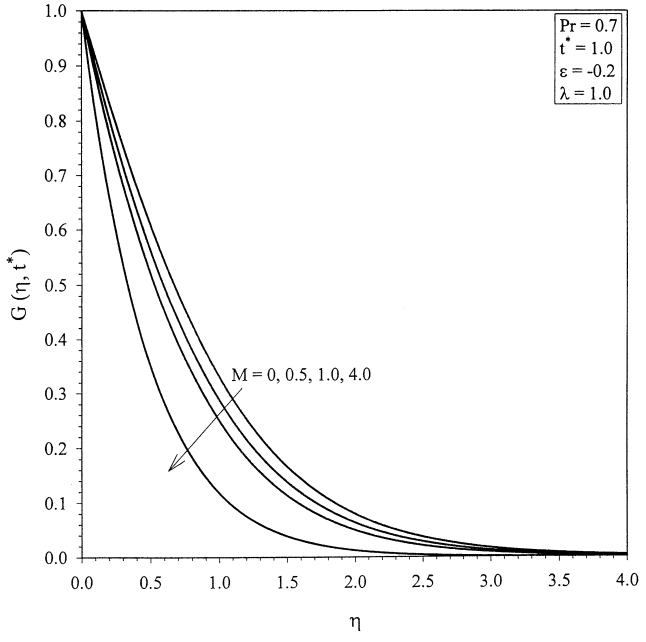

Fig. 10. Effect of M on velocity profiles G (η, t*) for φ(t*) = 1 + εt^{*2}, $\varepsilon = -0.2$

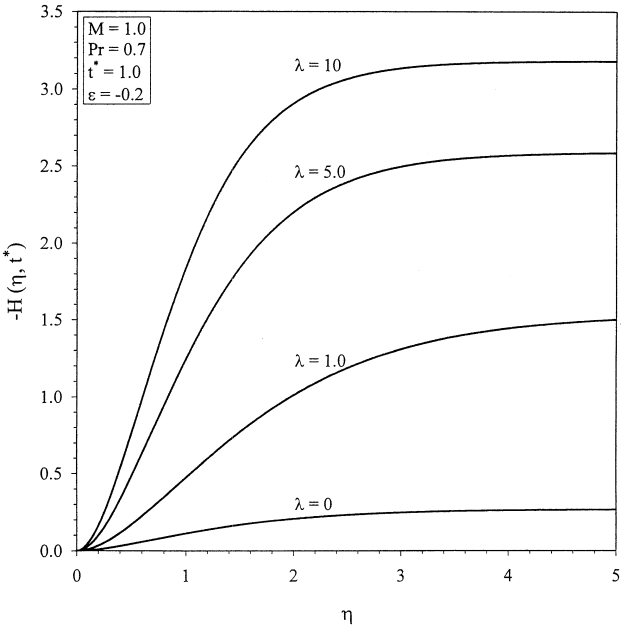

Fig. 12. Effect of λ on velocity profiles −H (η, t*) for (φt*) = 1 + εt^{*2}, $\varepsilon = -0.2$

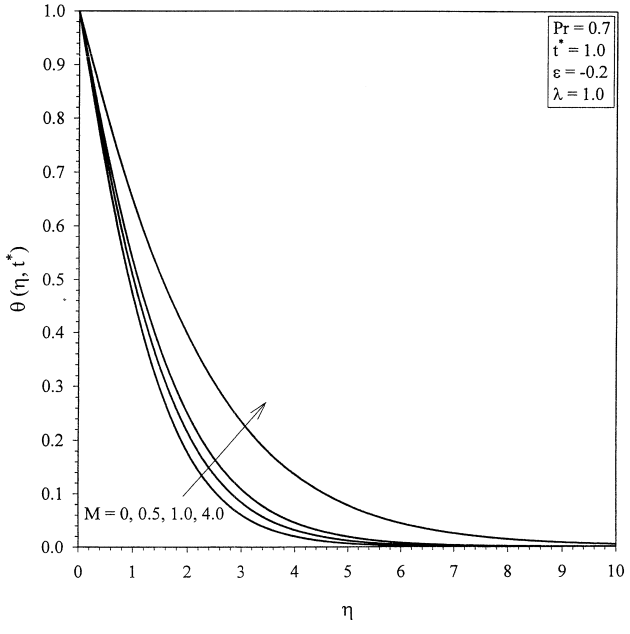

Fig. 11. Effect of M on temperature profiles θ (η, t*) for φ(t*) = 1 + εt^{*2}, $\varepsilon = -0.2$

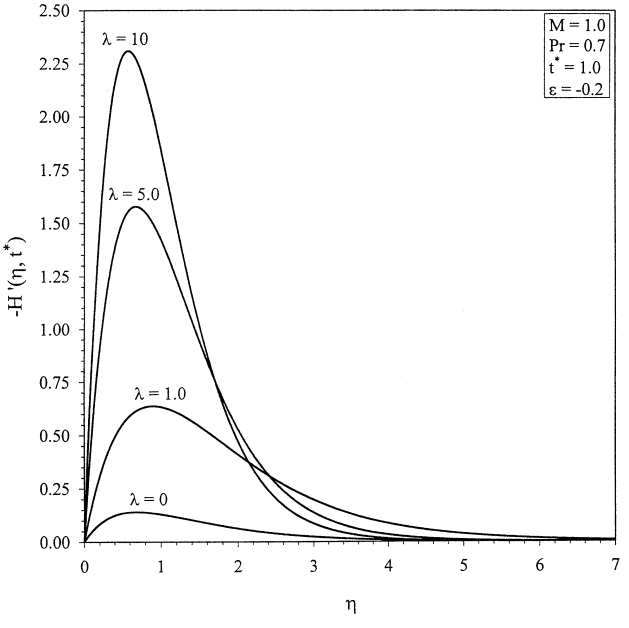

Fig. 13. Effect of λ on velocity profiles −H′ (η, t*) for φ (t*) = 1 + εt^{*2}, $\varepsilon = -0.2$

temperature (θ) for φ(t*) = 1 + εt^{*2}, $\varepsilon = -0.2$, t* = λ = 1, Pr = 0.7, is shown in Figs.8, 9, 10, 11. It can be seen from these figures that the velocities (H, H′, G) decrease with increasing M, but the temperature (θ) increases. The reason for this trend has been explained earlier.

The effect of the buoyancy λ on the velocity and temperature profiles (H, H′, G, θ) for φ(t*) = 1 + εt^{*2}, $\varepsilon = -0.2$, t* = M = 1 Pr = 0.7, is presented in Figs.12, 13, 14, 15. Since the buoyancy parameter λ accelerates the fluid in the buoyancy layer, both the momentum and the thermal boundary layers are reduced. This enhances the normal and tangential velocities (H, H′), but reduces the azimuthal velocity (G) and the temperature (θ).

5 Conclusions

The results indicate that the magnetic field significantly affects the velocity components and these, in general,

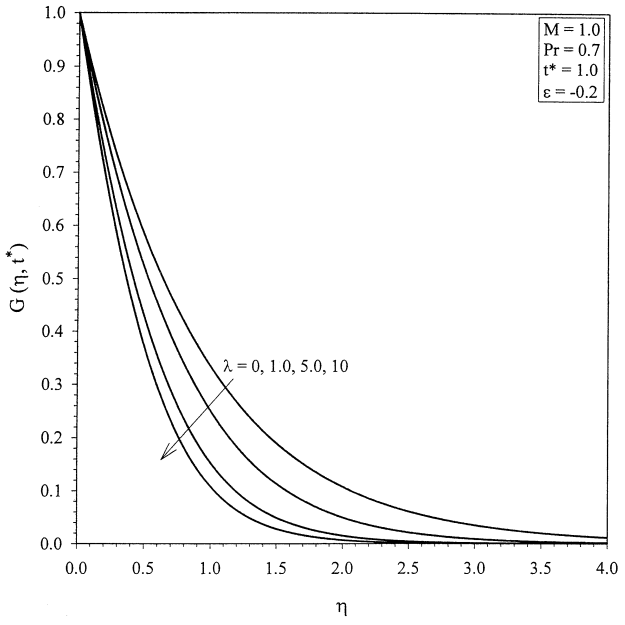

Fig. 14. Effect of λ on velocity profiles G (η, t*) for $\varphi(t^*) = 1 + \varepsilon t^{*2}$, $\varepsilon = -0.2$

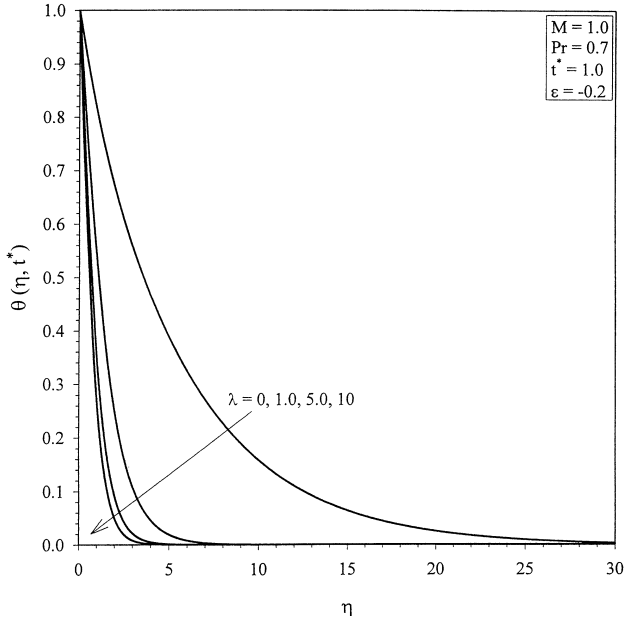

Fig. 15. Effect of λ on temperature profiles θ (η, t*) for $\varphi(t^*) = 1 + \varepsilon t^{*2}$, $\varepsilon = -0.2$

decrease with an increasing magnetic field, whereas the temperature increases. The skin friction coefficient in the tangential direction and the Nusselt number decrease with increasing magnetic field, but the skin friction in the circumferential direction increases. The buoyancy force enhances the skin-friction coefficients and the Nusselt number. The effect of the decreasing angular velocity on the velocity and the temperature fields is not the a mirror reflection of the increasing angular velocity.

References

1. Hickman KCD (1957) Centrifugal boiler compression still. Ind Eng Chem 49: 786–800
2. Ostrach S; Brown WH (1958) Natural convection inside a flat rotating container. NACA TN 4323
3. Dorman LA (1963) Hydrodynamic Resistance and the Heat Loss of Rotating Solids (Trans. by N Kemmer). Oliver and Boyd, Edinburgh
4. Kreith F (1968) Convective heat transfer in rotating systems. Advances in Heat Transfer (Eds. T.V. Irvine and J.P. Hartnett). 5: 129–251
5. Sparrow EM; Gregg JL (1959) Heat transfer from a rotating disk to fluids of any Prandtl number. J Heat Transfer 81: 249–251
6. Hartnett JP (1959) Heat Transfer from anon-isothermal disk rotating in still air. J Appl Mech 26: 672–673
7. Tien CL; Tsuji IJ (1965) A theoretical analysis of laminar forced flow and heat transfer about a rotating cone. J Heat Transfer 87: 184–190
8. Koh TCY; Price JF (1967) Nonsimilar boundary layer heat transfer of a rotating cone in forced flow. J Heat Transfer 89: 139–145
9. Hartnett JP; Deland EC (1961) The influence of Prandtl number on the heat transfer from rotating non-isothermal disks and cones. J Heat Transfer 83: 95–96
10. Sparrow EM; Cess RD (1962) Magnetohydrodynamic flow and heat-transfer about a rotating disk. J Appl Mech 29: 181–187
11. Tarek MA; Mishkawg El; Hazem AA; Adel AM (1998) Asymptotic solution for the flow due to an infinite rotating disk in the case of small magnetic field. Mech Res Comm 25: 271–278
12. Lee M; Jeng DR; Dewitt KJ (1978) Laminar boundary layer transfer over rotating bodies in forced flow. J Heat Transfer 100: 496–502
13. Wang CY (1990) Boundary layers on rotating cones, disks and axisymmetric surfaces with concentrated heat source. Acta Mechnica 81: 245–251
14. Hering RG; and Grosh RH (1963) Laminar combined convection from a rotating cone. ASME J Heat Transfer 85: 29–34
15. Himasekhar K; Sarma PK; Janardhan K (1989) Laminar mixed convection from a vertical rotating cone. IntComm Heat Mass Transfer 16: 99–106
16. Thacker WL; Watson LT; Kumar SK (1990) Magnetohydrodynamic free convection from a disk rotating in a vertical plane. Appl Math Modelling 14: 527–535
17. Ece MC (1992) An initial boundary layer flow past a translating and spinning rotational symmetric body. J Eng Math 26: 415–428
18. Ozturk A; Ece MC (1995) Unsteady forced convection heat transfer from a translating and spinning body. J Heat Transfer 117: 318–323
19. Blottner FG (1970) Finite-dierence method of solution of the boundary layer equations. AIAA J 8: 193–205
20. Eringen AC; Maugin GA (1990) Electrodynamic of Continua, Vol 2: Springer Verlag, Berlin